

UDC 661.666.4; 535.361

DOI: 10.15372/ChUR20160419

Optical Properties of Soot Simulation and Experimental Measurements for the Application in Special Devices

A. A. ZVEKOV¹, O. S. EFIMOVA¹, A. P. NIKITIN¹, I. YU. LISKOV¹, D. R. NURMUKHAMETOV¹, B. P. ADUEV¹, A. V. KALENSKII² and Z. R. ISMAGILOV¹

¹*Institute of Coal Chemistry and Material Science, Federal Research Center of Coal and Coal Chemistry, Siberian Branch, Russian Academy of Sciences, Kemerovo, Russia*

E-mail: zvekovaa@gmail.com

²*Kemerovo State University, Kemerovo, Russia*

Abstract

The absorption and scattering efficiencies, albedo and anisotropy factor values were calculated for soot particles in water and pentaerythritol tetranitrate media for different radii in terms of Mie theory. The main features of the calculation results include (i) the domination of absorption over scattering and (ii) the change of attenuation dependence on the wavelength trend at particle's radius about 150 nm. For smaller particles the attenuation efficiency decreases with wavelength increasing while for bigger ones the trend is just opposite. The soot particles in the experimental part of the work were characterized with dynamic light scattering. The obtained size-distribution is fit well with log-normal distribution having particles' radius expected value 183 nm. The spectra of total transmittance, ballistic transmittance and diffuse reflectance were measured for studied soot suspension in water. It was shown that the total transmittance does not depend significantly on the wavelength while the diffuse transmittance decreases twice with the wavelength increasing. It is concluded that the calculation results qualitatively agree with the experimental data if the typical particle's radius is twice smaller than one obtained with dynamic light scattering method. The possible applications of obtained optic properties of soot particles for special devices including optic detonator cups are discussed.

Keywords: soot, Mie theory, simulation, experimental measurement, diffuse reflectance spectroscopy

INTRODUCTION

The optic properties of carbon black and soot particles play a crucial part in the Earth climate, since such particles are able to efficiently absorb solar radiation making the atmosphere heat [1]. Depending on the altitude this effect could make the global warming or cooling as one feels the near-ground temperature only. Apart from this harmful influence, the light absorption by carbon black or soot particles is an essential process in light limiting devices that use their suspensions [2–4]. In [5, 6] the addition of soot to explosive substances were suggested in order to

increase their sensitivity to laser irradiation. The significant laser energy threshold value diminishing accompanied with substantial sample diffuse reflectance decreasing was achieved in [5]. The authors of [6] found out that pentaerythritol tetranitrate containing soot additive became sensitive to laser pulses of millisecond duration. All these examples show that the optic properties of soot are essential in many applications and need to be researched. The objectives of the present paper are: (i) calculation of soot optic properties in terms of Mie theory, (ii) experimental study of optic spectra for a well-characterized soot suspension sample.

METHODOLOGY

The interaction of the soot particles and the electromagnetic radiation is traditionally described by using the absorption efficiency (Q_{abs}) and scattering efficiency factors (Q_{sca}). These dimensionless parameters are equal to the ratio of the particle cross-section and its geometrical cross-section $Q = \sigma/\sigma_g$. The Q_{abs} was calculated in terms of Mie theory as the difference of the attenuation efficiency (Q_{ext}) and scattering efficiency factors (Q_{sca}) [7–9].

The main parameters of the theory are the complex refractive index (m_i) of the material of interest, which depends on the wavelength of the incident light (λ), and the refractive index of the media (m_0) [9]. These data in the range 400–1000 nm were taken from [10]. The data used are typical for carbon particles and

comparable to presented in other sources [11, 12]. The range of particles radii studied $10 < R < 300$ nm is concerned on their possible application to optic initiation systems or light limiting devices [1–6].

In the experimental part of the present work we prepared soot suspension samples in water. The suspension was ultrasonificated in order to obtain the reproducible particle sizes. The power of the ultrasound source was 50 W. The ultrasonification time was higher than 15 min. The suspension transferred to the cuvettes with a pipette. If the suspension began to coagulate inside the pipette we treated it in the ultrasonic bath one more time.

The size-distribution was studied using Malvern Zetasizer in a 1 cm disposable plastic cuvette. The optic properties were researched with a Shimadzu UV-2450 spectrometer

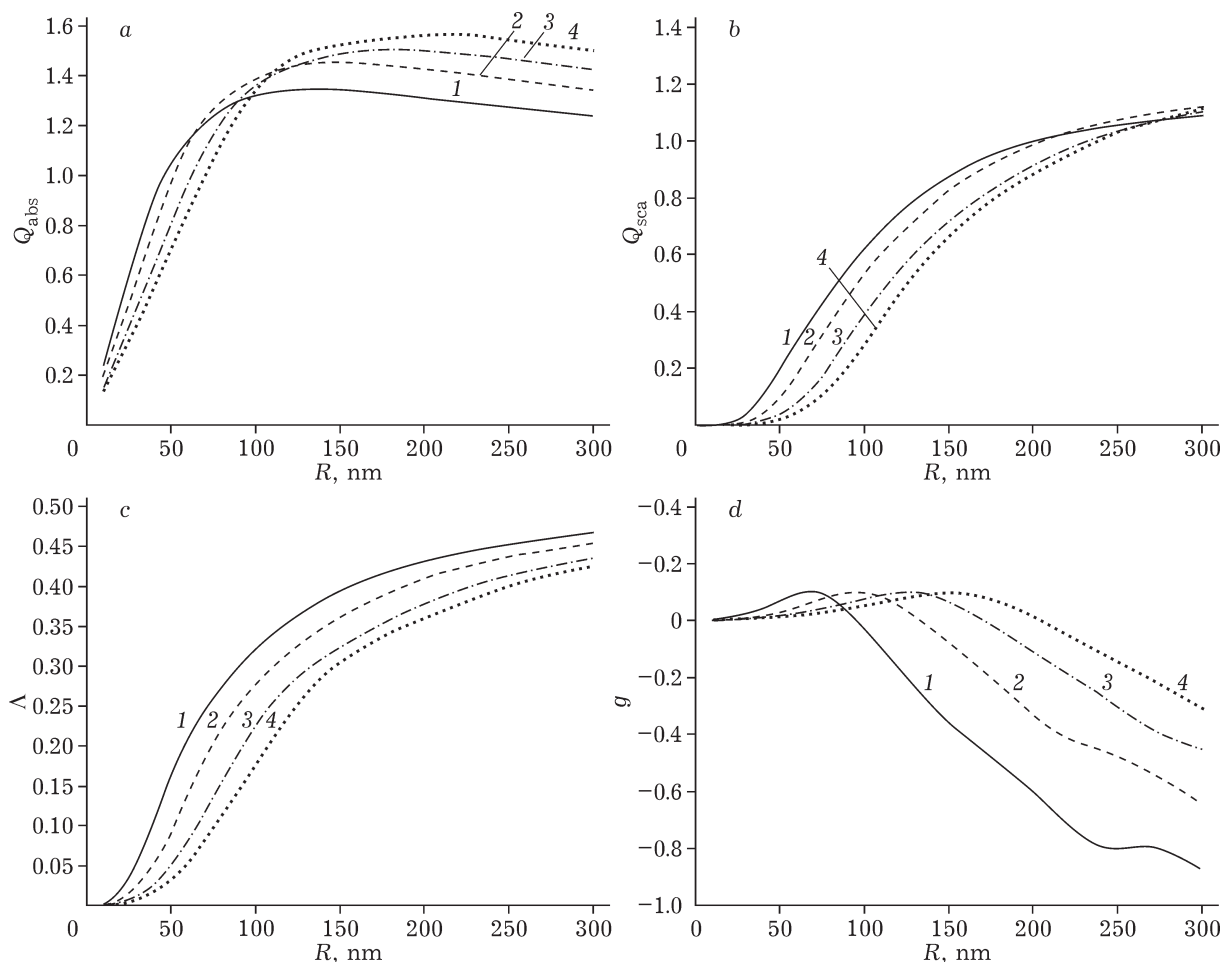


Fig. 1. Calculated dependencies of absorption (a) and scattering (b) efficiency factors, single scattering albedo (c) and the anisotropy factor (d) for soot particles in water at the wavelength 400 (1), 600 (2), 800 (3) and 1000 nm (4).

equipped with an integrating sphere. It allowed us to measure ballistic transmittance, total transmittance, diffuse transmittance and diffuse reflectance spectral dependencies. The glass cuvette with 1 mm optic path length and 3 mm walls was filled with the soot suspension. The transmittance was measured using another cuvette filled with water as a reference sample. The spectral slit width was 5 nm. We used a 5 mm square mask providing 2 mm square beam on the sample surface when the transmittance was measured.

RESULTS AND DISCUSSION

The results of soot particle optical properties calculation in terms of Mie theory are presented in Fig. 1. The calculations were done at four wavelength values of 400, 600, 800 and 1000 nm. The absorption efficiency (see Fig. 1, *a*) increases with the particles radius increasing in the range of small radii. The dependence is close to the linear one which means that the Rayleigh's scattering limit is matched well. The maximum position depends on the wavelength. For instance at $\lambda = 400$ nm the particles with radius 135 nm performs the maximum absorption efficiency equal 1.346. At the wavelength 1000 nm the maximum shifts to the radius value 213 nm though its amplitude does not change much (1.564). The persistence of the Rayleigh's scattering limit is seen as the dependence $Q_{\text{sca}}(R)$ could be described with expression $\text{const} \cdot R^4$ for $R/\lambda < 0.2$ (see Fig 1, *b*). The scattering efficiency values are lower than the absorption efficiencies in all the studied range of radii and wavelengths. For that reason, the albedo values are lower than 0.5 (see Fig. 1, *c*). The albedo increases with the radius increasing and wavelength decreasing. Though the maxima on the $Q_{\text{sca}}(R)$ dependence are observed outside the plot range, it is clear that absorption efficiency decreasing for R bigger that 200 nm is accompanied with scattering efficiency increasing. It makes the attenuation efficiency almost independent on the particles radius in that range. The interesting peculiarity is concerned on the wavelength dependence of the attenuation efficiency. For the particle radii less than 150 nm the wavelength increasing makes the attenua-

tion efficiency decrease while for bigger particles the trend is just opposite. In the radius range 120–200 nm the attenuation efficiency factor changes less than 10 % in the spectral range 400–1000 nm.

The calculated scattering anisotropy factor, which is the average cosine of the scattering angle is depicted in Fig. 1, *d*. The scattering anisotropy tends to zero in the limit $R \rightarrow 0$ as it should be for the Rayleigh scattering. Then, one can notice its increasing with the particle's radius. The trend changes then to the diminishing. The negative values mean that the back-scattering dominates. The radius values corresponding to the anisotropy factor abscissa axis crossing correlate with the maximum positions on the $Q_{\text{abs}}(R)$ dependence.

The size distribution of soot particles in the experimentally studied suspension determined with the dynamic light scattering method is shown in Fig. 2. The measurements were done for the suspension sample containing 37.5 $\mu\text{g}/\text{mL}$ of soot. The distribution is single-mode with typical full width at half maximum 140 nm. It is fitted well with log-normal distribution:

$$w_{\text{norm}} = \frac{1}{\sqrt{2\pi}\sigma R} \exp\left[-\frac{(\ln R - \mu)^2}{\sigma^2}\right] \quad (1)$$

The obtained fitting parameters were $\mu = 5.01$ and $\sigma = 0.446$. The distribution mode is

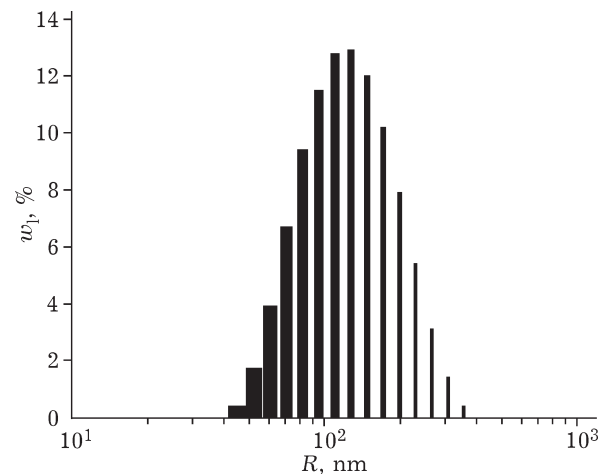


Fig. 2. Soot particles size-distribution obtained with dynamic light scattering method.

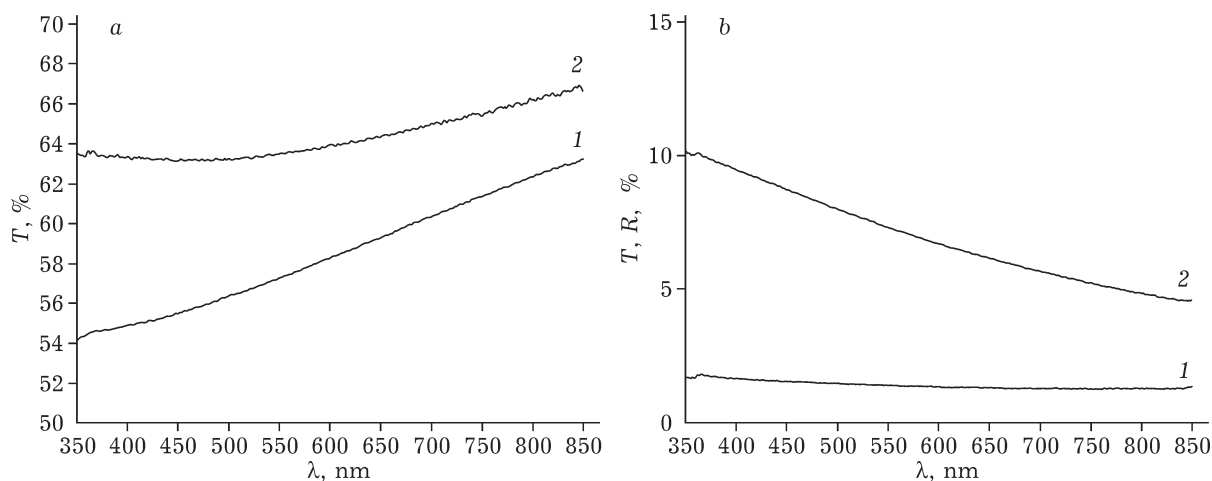


Fig. 3. Measured optical properties of soot suspension: *a* – ballistic transmittance (1) and total transmittance (2); *b* – diffuse reflectance (1) and diffuse transmittance (2).

123 nm, the median is 150 nm and the radius mean value is 183 nm.

It worth mentioning that soot and carbon black particles are usually considered aggregated when they are dispersed in a medium [11–14]. The aggregation in liquids is dealt with lyophobic interactions [14]. Significant aggregation observed typically when soot is formed in the gas phase [12, 13]. The hydrodynamic radius obtained with dynamic light scattering approach should be associated with aggregates including possible solvation atmosphere.

The measured spectral dependencies of ballistic transmittance and total transmittance, as well as diffuse transmittance and diffuse reflectance are shown in Fig. 3, *a* and *b*, correspondingly. The suspension concentration was 49 μg/mL. The spectral range was limited by the glass cuvette transparency range. Both the measured values of total transmittance and its ballistic component decreases as the wavelength become lower though this decreasing seems more evident for the ballistic component. The ratio of optical density corresponding to the ballistic transmittance at 350 and 850 nm is 1.33. The sum of diffuse transmittance and ballistic transmittance matches the total transmittance well in the entire studied wavelength region. The diffuse transmittance decreases with the wavelength increasing. At the same time the diffuse reflectance does not change much in the studied wavelength range being lower than the diffuse transmittance values.

Comparing the calculated (see Fig. 1) and experimentally determined (see Fig. 3) optical properties one is able to see that they partly agree. According to the dynamic light scattering measurements the typical particles' radius is about 150 nm, which matches the area where the attenuation efficiency factor does not depend on the wavelength significantly. The ratio of optic densities at 350 and 850 nm is close to the ratio of attenuation efficiency factors calculated for the radius of the particles 75 nm. The measured diffuse transmittance decreases when the wavelength increases while the diffuse reflectance keeps almost constant. It correlates with calculated scattering efficiency decreasing with wavelength increasing evident from Fig. 1, *b*. On the other hand diffuse transmittance is higher than the diffuse reflectance. Their difference decreases when the wavelength becomes higher (see Fig. 2, *b*). The ratio of diffuse transmittance and diffuse reflectance gives the information on the scattering anisotropy sign. When diffuse reflectance is higher than diffuse transmittance in the limit of single scattering, the scattering anisotropy is negative, which is not the case (see Fig. 3). The ratio of diffuse transmittance and diffuse reflectance diminishes with the wavelength evidencing the decreasing of scattering anisotropy factor. Comparing to the calculation results (see Fig. 1, *d*), this trend is typical for nanoparticles having radii about 70 nm.

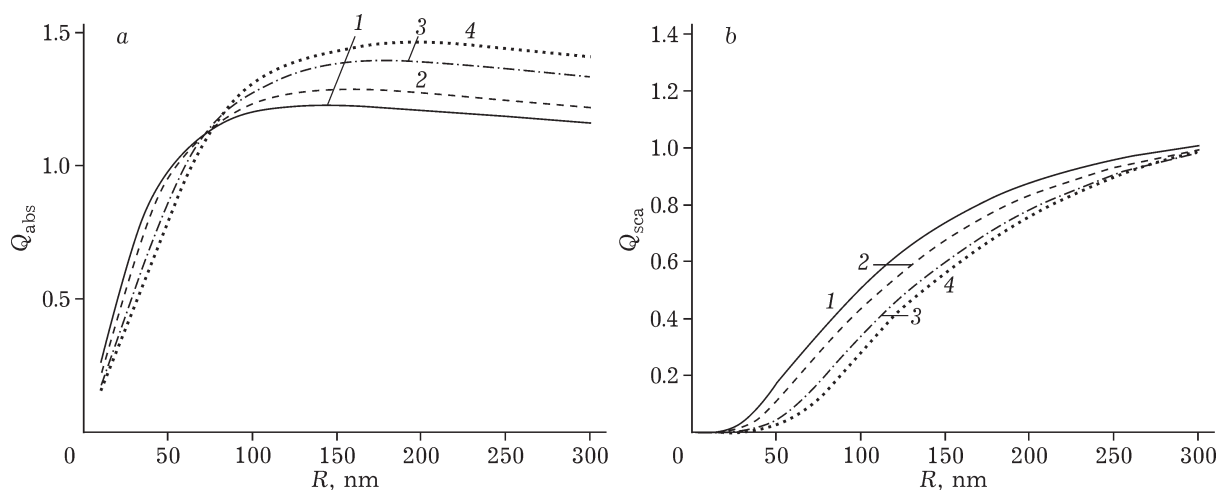


Fig. 4. Calculated dependencies of absorption (a) and scattering (b) efficiency factors for soot particles in PETN at the wavelength 400 (1), 532 (2), 800 (3) and 1000 nm (4).

Thus, the calculated optic properties correspond to the experimentally measured values if one assumes that the particle size is twice smaller than hydrodynamic radius. This difference could be concerned on the particle aggregation or formation of solvent layer around the particle moving together with it. The typical aggregates have non-spherical shape. The net scattering pattern for such aggregates should be nearly isotropic due to angular averaging. On the other hand, non-spherical particles usually appear as bimodal size distribution when it is determined with dynamic light scattering technics. For the reasons listed it seems that aggregation is not the cause of the deviation of hydrodynamic radius from the optic one. The solvent ordering around the particle could be concerned on the side groups or carbon layers disrupted from the main soot particle.

We performed the calculation of optical properties of soot including absorption and scattering efficiency factors in the matrix of pentaerythritol tetranitrate (PETN). The results are presented in Fig. 4. The higher refractive index of the medium (1.54) makes the dependencies a bit different from shown in Fig. 1 conserving the main features. The maximum absorption efficiency factor equal to 1.226 is observed for particle radius 141 nm at the wavelength 400 nm. Its position corresponds to the values calculated for metal nanoparticles in the same matrix. The scattering efficiency factor varies less in PETN matrix than in water in the stud-

ied wavelength range. The calculations were also performed at the wavelength 532 nm corresponding to the second harmonics of the neodymium laser. The absorption efficiency in that case keeps almost constant for particle radii higher than 100 nm making the difference to the results obtained for noble metal nanoparticles [8]. The calculated albedo values are significantly lower than experimentally determined for aluminum nanoparticles [15] or calculated for cobalt nanoparticles [16] in PETN and cyclonite matrixes respectively.

Relatively high absorption efficiencies make soot particles a prospective additive to explosive substances that allow one to increase their sensitivity to laser irradiation. One of the advantages readily seen from Fig. 4 is insignificant variation of the absorption efficiency in the wavelength range 40–1000 nm. For that reason the device performance could be approximately independent on the wavelength of the laser. A similar advantage appears when one uses soot suspensions as a non-linear light attenuation device [17]. The main problem on the way is to develop an approach of the soot particles mixing with explosive giving an opportunity to prepare homogeneous samples with reproducible properties.

CONCLUSION

The optical properties of soot particles in water and pentaerythritol tetranitrate media

were calculated for various radii in terms of Mie theory. The absorption process dominates over scattering for all the studied radii and wavelength values. The soot suspension in water was researched using dynamic light scattering method and visible spectroscopy. It was shown that the optical properties corresponded to the particle size twice less than determined with dynamic light scattering technics.

The efficient light absorption makes soot a prospective dopant for optical detonator cup developed on the basis of secondary explosives. An additional advantage is related to an insignificant dependence of the absorption efficiency factor on the wavelength that allows using different lasers with one cup composition. The same advantage is essential for the development of non-linear light attenuation devices.

Acknowledgements

The work was partly supported by the grant of Russian Federation President (MK-4331.2015.2), Russian Foundation for Basic Research (project No. 16-33-00510 mol_a) and Ministry of Education and Science of the Russian Federation (governmental project 3606, task 2014/64).

REFERENCES

- 1 Matvienko G. G., Belan B. D., Panchenko M. V., Romanovskii O. A., Sakerin D. M., Kabanov S. M., Turchinovich S. A., Turchinovich Y. S., Eremina T. A., Kozlov V. S., Terpugova S. A., Pol'kin V. V., Yausheva E. P., Chernov D. G., Zhuravleva T. B., Bedareva T. V., Odintsov S. L., Burlakov V. D., Nevzorov A. V., Arshinov M. Y., Ivlev G. A., Savkin D. E., Fofonov A. V., Gladkikh V. A., Kamardin A. P., Balin Y. S., Kokhanenko G. P., Penner I. E., Samoilova S. V., Antokhin P. N., Arshinova V. G., Davydov D. K., Kozlov A. V., Pestunov D. A., Rasskazchikova T. M., Simonenkov D. V., Sklyadneva T. K., Tolmachev G. N., Belan S. B., Shmargunov V. P., Kozlov A. S., and Malyshkin S. B., *Atmos. Measur. Techn.*, 8, 10 (2015) 4507.
- 2 Mansour K., Soileau M. J., Van Stryland E. W., *J. Optic. Soc. America B*, 9, 7 (1992) 1100.
- 3 P. Aloukos, I. Papagiannouli, A. Bourlinos, Zboril R., Couris S., *Opt. Express*, 22, 10 (2014) 12013.
- 4 Belousova I. M., Danilov O. B., Sidorov A. I., *J. Opt. Technol.*, 76, 4 (2009) 223.
- 5 Aleksandrov E. I., Voznyuk A. G., Tsipilev V. P., *Combustion, Explosion, and Shock Waves*, 25, 1 (1989) 1.
- 6 Aluker E. D., Zverev A. S., Krechetov A. G., Mitrofanov A. Y., Terentyeva A. O., *Rus. J. Phys. Chem. B*, 8, 5 (2014) 687.
- 7 Kalenskii A. V., Zvekoy A. A., Anan'eva M. V., Zykoy I. Yu., Kriger V. G., and Aduoy B. P., *Combustion, Explosion, and Shock Waves*, 50, 3 (2014) 333.
- 8 Kalenskii A. V., Zvekoy A. A., Nikitin A. P., *Opt. Spectrosc.*, 118, 6 (2015) 978.
- 9 Aduoy B. P., Nurmukhametov D. R., Belokurov G. M. and Nelyubina N. V., *Tech. Phys.*, 59, 9 (2014) 1387.
- 10 Bloh A. G., *Thermal Eng.*, 4, 7 (1964) 16.
- 11 Soewono A., Rogak S. N., *Aerosol Sci. Technol.*, 47, 3 (2013) 267.
- 12 Radney J. G., You R., Ma Xiaofei, *J. Environ. Sci. Technol.*, 48 (2014) 3169.
- 13 Mikhailov E. F., Vlasenko S. S., *Izv. Atmos. and Oceanic Phys.*, 43, 2 (2007) 181.
- 14 Huaxin Xue, Alexei F. Khalizov, Lin Wang, Jun Zheng and Renyi Zhang, *Phys. Chem. Chem. Phys.*, 11 (2009) 7869.
- 15 Aduoy B. P., Nurmukhametov D. R., Zvekoy A. A., Nelyubina N. V., Belokurov G. M. Kalenskii A. V., *Instrum. Exp. Tech.*, 58, 6 (2015) 765.
- 16 Zvekoy A. A., Kalenskii A. V., Aduoy B. P., Ananyeva M. V., *J. Appl. Spectr.*, 82, 2 (2015) 213.
- 17 Belousova I. M., Mironova N. G., Scobelev A. G., Yur'ev M. S., *Optics Commun.*, 235 (2004) 445.

UDC 661.666.4; 535.361

DOI: 10.15372/KhUR20160419

Моделирование и экспериментальное измерение оптических свойств сажи для некоторых приложений

А. А. ЗВЕКОВ¹, О. С. ЕФИМОВА¹, А. П. НИКИТИН¹, И. Ю. ЛИСКОВ¹, Д. Р. НУРМУХАМЕТОВ¹, Б. П. АДУЕВ¹, А. В. КАЛЕНСКИЙ², З. Р. ИСМАГИЛОВ¹

¹Институт углекислоты и химического материаловедения
Федерального исследовательского центра угля и углекислоты Сибирского отделения РАН,
Кемерово, Россия

E-mail: zvekova@gmail.com

²Кемеровский государственный университет, Кемерово, Россия

E-mail: kriger@kemsu.ru

Аннотация

В рамках теории Ми рассчитаны значения факторов эффективности поглощения и рассеяния, альбедо однократного рассеяния и фактора анизотропии рассеяния при варьировании радиуса частиц сажи в воде и пентаэритрите тетрагидрате. Анализ результатов расчетов показал что: 1) поглощение преобладает над рассеянием; 2) при радиусах частиц сажи порядка 150 нм происходит смена знака производной фактора эффективности ослабления по длине волны. Для частиц меньших радиусов фактор эффективности ослабления уменьшается при росте длины волны, и возрастает при больших. В экспериментальной части работы использовалась суспензия частиц сажи в воде, охарактеризованная методом динамического рассеяния света. Полученное распределение по радиусам хорошо описывается логнормальным законом с математическим ожиданием 183 нм. Для образца суспензии сажи измерены спектральные зависимости коэффициентов полного пропускания, коллимированного пропускания и диффузного отражения. Показано, что коэффициент полного пропускания практически не зависит от длины волны, тогда как коэффициент диффузного пропускания уменьшается вдвое при росте длины волны в видимой области. Сделан вывод, что для согласования результатов расчетов и оптических измерений требуется, чтобы характерный радиус наночастиц был в два раза меньше, чем, определенный методом динамического рассеяния света. Обсуждаются возможные приложения результатов для использования сажи в различных исполнительных устройствах, включая оптические детонаторы.

Ключевые слова: сажа, теория Ми, моделирование, экспериментальные измерения, спектроскопия диффузного отражения

